Archives of Current Research International

Volume 25, Issue 5, Page 427-444, 2025; Article no.ACRI.135820
ISSN: 2454-7077

Improved Lead and Cadmium Adsorption from Wastewater Using Thermo-chemically Activated Bentonite: Equilibrium, Kinetics, and Thermodynamics

Madhumonti Saha [a,b*], Pabitra Kumar Biswas [a], Jayanta Kumar Saha [b], Abhijit Sarkar [b], Sangeeta Lenka [b], M. Vassanda Coumar [b] and Dinesh Kumar Yadav [b]

[a] Department of Soil Science and Agricultural Chemistry, Institute of Agriculture, Visva Bharati University, Sriniketan 731236, India.
[b] Division of Environmental Soil Science, ICAR-Indian Institute of Soil Science, Bhopal 462038, India.

Authors' contributions

This work was carried out in collaboration among all authors. Author MS conceptualized and investigated the study, edited and wrote the original draft of the manuscript. Author PKB supervised and reviewed the study. Author JKS supervised the study and did data curation. Author AS did the formal analysis, data validation, reviewed and edited the manuscript. Author DKY and MVC searched for resources and edited the manuscript. Author SL reviewed and characterized the techniques. All authors read and approved the final manuscript.

Article Information

DOI: https://doi.org/10.9734/acri/2025/v25i51222

Open Peer Review History:
This journal follows the Advanced Open Peer Review policy. Identity of the Reviewers, Editor(s) and additional Reviewers, peer review comments, different versions of the manuscript, comments of the editors, etc are available here: https://pr.sdiarticle5.com/review-history/135820

Original Research Article

Received: 05/03/2025
Accepted: 07/05/2025
Published: 12/05/2025

**Corresponding author: Email: madhumonti2609@gmail.com;*

Cite as: *Saha, Madhumonti, Pabitra Kumar Biswas, Jayanta Kumar Saha, Abhijit Sarkar, Sangeeta Lenka, M. Vassanda Coumar, and Dinesh Kumar Yadav. 2025. "Improved Lead and Cadmium Adsorption from Wastewater Using Thermo-Chemically Activated Bentonite: Equilibrium, Kinetics, and Thermodynamics". Archives of Current Research International 25 (5):427-44. https://doi.org/10.9734/acri/2025/v25i51222.*

ABSTRACT

Aims: The effective treatment of wastewater contaminated with toxic metals such as lead (Pb) and cadmium (Cd) is vital for environmental sustainability and safe agricultural reuse as they are poisonous and may build up in the food chain, which can harm the ecosystem and cause health issues.

Study Design: This study investigates the efficacy of thermo-chemically activated bentonite (Ac-Ben) compared to raw bentonite (Ben) for the removal of Pb(II) and Cd(II) from aqueous solutions using completely randomized design (CRD) in triplicates.

Place and Duration of Study: Ac-Ben was synthesized and subsequent experiments were conducted at the Environmental Soil Science laboratory of ICAR-Indian Institute of Soil Science, Bhopal during 2023-2024.

Methodology: Ac-Ben was synthesized by acid treatment of bentonite, and its enhanced physicochemical properties were confirmed via X-ray diffraction (XRD), scanning electron microscopy-cum-energy dispersive X-ray spectroscopy (SEM-EDX), Fourier transform infrared spectroscopy (FTIR), specific surface area analysis, and point of zero charge (PZC) measurements. Batch adsorption experiments evaluated the effect of contact time, pH, adsorbent dosage, temperature, and initial metal concentrations.

Results: The adsorption process could be optimized with 60 min shaking time, solution pH = 5, 10 g L^{-1} adsorbent dose and 298 K reaction temperature. The pseudo-first-order kinetic model (R^2 ranges 0.996 to 0.999) and Langmuir isotherm best described the adsorption behavior, with Ac-Ben exhibiting higher maximum adsorption capacities (127.2 mg g^{-1} for Pb(II), 132.2 mg g^{-1} for Cd(II)) than Ben. Adsorption was spontaneous and exothermic, with reduced efficiency at elevated temperatures. Mechanistic analysis suggested that physisorption, electrostatic attraction, and ion exchange were the primary mechanisms. Ac-Ben maintained >85 % removal efficiency after three regeneration cycles, confirming its potential as a sustainable, efficient, and reusable adsorbent for heavy metal remediation from wastewater.

Conclusion: Thermo-chemical activation markedly enhances bentonite's affinity for Pb(II) and Cd (II). Owing to its abundance, low cost, and re-usability, Ac-Ben is a promising adsorbent for decentralized wastewater treatment, supporting SDG 6 on clean water.

Keywords: Bentonite; thermo-chemical activation; adsorption; kinetics; wastewater; thermodynamics.

1. INTRODUCTION

Annually approximately 40 billion cubic meters (BCM) of wastewater is generated and released due to advancement of urbanization, civilization and industrialization (Ungureanu et al. 2020). Industrial sectors share 20-30% and households share 70-80% of total wastewater generated and released in the environment which contaminate approx. 5500 BCM fresh water annually (Minhas et al. 2022). By 2025, it is estimated that two thirds of the world's population would experience water scarcity, and global ecosystems could suffer far more as a result of contamination of the global food chain (Hussain et al. 2019). "Despite all of these worries, wastewater irrigation lowers the cost of cultivation and improves the prospects for millions of farmers in peri-urban areas to make a living" (Minhas et al. 2022). A comprehensive, integrated, and multifaceted coordination among public health engineers, agronomists, hydrobiologists, medical professionals, and farming communities is necessary for the development of appropriate methodologies for the safe use of wastewater over an extended period of time.

Lead (Pb) and cadmium (Cd), two toxic trace elements that can be found in water, are fatal to humans. Prolonged exposure to Pb(II) (above 0.05 mg L^{-1} in drinking water) has been linked to a number of health issues, including elevated blood pressure, impaired renal function, reproductive disorders, and an increased risk of hypertension (Nag and Cummins 2022). Additionally, "irrigation water containing 5 mg L^{-1} of Pb(II) has also been linked to health problems. Similarly, prolonged exposure to low levels of Cd(II) (above 0.005 mg L^{-1} in drinking water) can change the composition of bones, lower bone density, and pose other health problems to humans" (Khanam et al. 2020), high levels of Cd(II) (above 0.01 mg L^{-1}) in irrigation water can also prevent plants from growing. Both Pb(II) and Cd(II) are carcinogenic metals. Therefore, removal of both Pb(II) and Cd(II) from the wastewater is essential to meet the future water demand for agriculture and other uses.

Though wastewater treatment techniques like biodegradation, photo-oxidation, chemical oxidation, coagulation, ion exchange, membrane separation, adsorption etc. are available, but adsorption technology is most economically feasible and widely acceptable (Minhas et al. 2022). Researchers are now paying much attention to increase the adsorption capacity of different conventional and unconventional adsorbents through chemical or physical modification for better reusability of adsorbents, design flexibility, and robust working conditions. "Bentonite is an abundant and naturally occurring clay composed of hydrous aluminosilicates, which are blends of fine-grained earth minerals and metal oxides" (Sarkar et al. 2021). "This 2:1 layer structure of bentonite consists of an octahedral alumina sheet that fits between two opposing tetrahedral silica sheets. They are stacked in shelves, with spaces between them filled with exchangeable metal cations. Bentonite is often utilized as an adsorbent for the removal of metal ions due to its higher surface area, cation exchange ability, and adsorptive capacity for various pollutants (organic and inorganic)" (Mukhopadhyay et al. 2019). In order to increase its surface modification, adsorption capacity and cation exchange capacity (CEC), activation is used for significant chemical and mineralogical changes in bentonite (Babaki et al. 2008). Acid activation of bentonite is well known and researchers have concentrated on different aspects like removal dye, heavy metals with acid activated bentonites (Anna et al. 2014). Xu et al. (2021) demonstrated that the humic acid-iron-columnar bentonite (HA-Fe-PILC) was an efficient and reusable adsorbent for Cd(II) and Pb(II) removal from wastewater.

In this study we have prepared activated bentonite (Ac-Ben) following thermo-chemical activation of bentonite, which is a new prospective for the heavy metal ions adsorption from aqueous solutions. The novelty of the present work is to prepare activated bentonite (Ac-Ben) and compare it with raw bentonite (Ben) for efficient adsorption of two toxic trace metals (Pb and Cd) from wastewater. Thus, we hypothesize that activation of bentonite will affect its adsorption performance for heavy metals. The aim of this study was to (1) study the Pb(II) and Cd(II) adsorption characteristics of novel acid-activated bentonite synthesized under different activator moduli, and (2) to investigate the conditions and mechanisms of Pb(II) and Cd(II) adsorption onto the adsorbents.

2. MATERIALS AND METHODS

2.1 Reagents and Materials

Raw bentonite (Ben) powder was procured from HiMedia Laboratories Pvt. Ltd., India. Analytical grade lead nitrate [$Pb(NO_3)_2$] and cadmium nitrate tetrahydrate [$Cd\ (NO_3)_2 \cdot 4H_2O$] were obtained from Merck India Ltd. Sulfuric acid (H_2SO_4) and other reagents were of analytical grade and used without further purification. Deionized water was used for all solution preparations.

2.2 Thermo-Chemical Activation of Bentonite

Activated bentonite (Ac-Ben) was synthesized through thermo-chemical treatment of raw bentonite. Initially, 400 g of Ben was dried at 105°C for 2 hours to remove moisture. The dried clay was then mixed with 2 *M* H_2SO_4 in a 1:2 (w/v) ratio and stirred manually (modified from Nwosu et al. 2019). The mixture was further agitated on a rotary shaker for 30 minutes, followed by heating at 80°C for 1 hour. The resultant slurry was cooled, repeatedly washed with distilled water until a neutral pH was attained, air-dried, ground, and sieved through a 100-mesh sieve to yield Ac-Ben. Experimental methodology is presented in Fig.1.

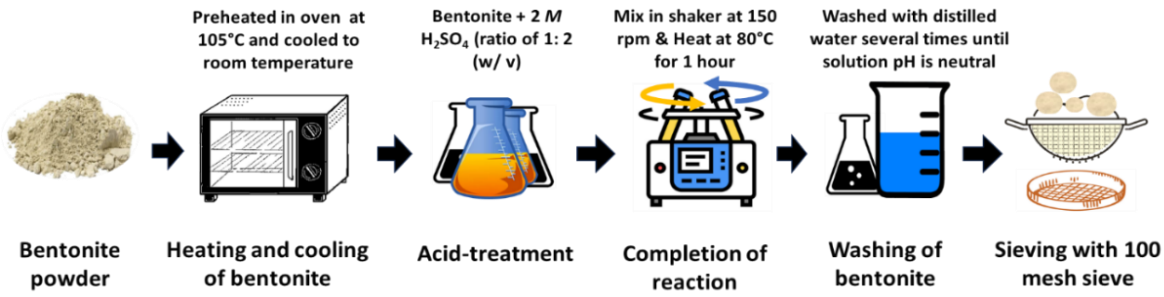

Fig. 1. Experimental methodology for the synthesis of the adsorbents (Ac-Ben) via thermo-chemical activation of pulverized bentonite

2.3 Characterization of Adsorbents

2.3.1 X-Ray Diffraction (XRD)

Crystalline structures were examined using a Philips PW 1710 X-ray diffractometer with Cu–Kα radiation (λ = 0.15418 nm). Scans were conducted between 4°–50° (2θ) at 0.025° s^{-1}.

2.3.2 SEM-EDX

Surface morphology and elemental composition were assessed using a JEOL JSM-5600 scanning electron microscope coupled with energy dispersive X-ray spectroscopy.

2.3.3 FTIR spectroscopy

Bond vibrations and functional groups before and after metal adsorption were analyzed using a Thermo Scientific Nicolet iS5 FTIR spectrometer, operating in the 4000–400 cm^{-1} range with 0.5 cm^{-1} resolution using KBr pellets.

2.3.4 Specific surface area

Determined via the ethylene glycol monoethyl ether (EGME) method, providing access to interlayer surface area more effectively than gas adsorption techniques (Carter et al.,1986).

2.3.5 Point of Zero Charge (pHPZC)

Estimated by the solid addition method. Adsorbents (50 mg) were added to 50 mL of 0.01 *M* or 0.1 *M* KNO_3 solution adjusted to initial pH values between 1 and 13. After 24 h equilibration, final pH values were measured to determine pHPZC (Gorgievski et al., 2013).

2.4 Batch Adsorption Experiments

2.4.1 Adsorbate preparation

Synthetic wastewater was prepared by diluting stock solutions (1000 mg L^{-1}) of Pb(II) and Cd(II) to desired concentrations.

2.4.2 Adsorption conditions

Batch experiments investigated the influence of various parameters, including contact time (5–360 min), pH (3–8), adsorbent dose (0–40 g L^{-1}), initial metal concentration (Pb: 0–200 mg L−1; Cd: 0–10 mg L^{-1}), and temperature (298–318 K). Each experiment was conducted in triplicate using 50 mL of metal solution with 10 g L^{-1} adsorbent and shaken at 150 rpm. After equilibrium, samples were centrifuged and filtered through Whatman No. 42 filter paper. Residual metal concentrations were measured using ICP-OES (Perkin Elmer Avio 560 Max).

2.5 Desorption and Reusability

Adsorbents saturated with Pb(II) and Cd(II) were treated with 0.2 *M* HCl and shaken for 30 min, followed by centrifugation. Recovered adsorbents were rinsed and reused in subsequent cycles. Adsorption efficiency was assessed over three cycles.

2.6 Adsorption Modelling and Analysis

The adsorption capacity (qt, mg g^{-1}) and removal efficiency (%) for Pb(II) and Cd(II) by Ben and Ac-Ben at equilibrium was calculated using Eq. 1 and Eq. 2.

$$q_t = [(C_0 - C_e)*V]/ M \quad (1)$$

$$R(\%) = [(C_0 - C_e)/ C0] \times 100 \quad (2)$$

Where C_0 and C_e is correspondingly initial and equilibrium adsorbate concentration (mg L^{-1}), V is total volume adsorbate (L), and M is the amount of adsorbent (g).

2.6.1 Adsorption kinetic models

Pseudo-first-order (Eq. 3), pseudo-second-order (Eq. 4), and Elovich (Eq. 5) kinetic models were applied to time-dependent adsorption data.

$$q_t = q_e (1-e^{k1t}) \quad (3)$$

$$q_t = ((q_e)^2 k_2 t)/ (1 + q_t k_2 t) \quad (4)$$

$$q_t = 1/\beta \ln(\alpha\beta t+1) \quad (5)$$

Where q_t and q_e are the amount of metal adsorbed (mg g^{-1}) at time t and at equilibrium, k_1 is the rate constant of the pseudo-first order (min^{-1}), t is the time (min), k_2 is the rate constant of the pseudo-second order (g mg^{-1} min^{-1}), α is the initial rate of adsorption (mg g^{-1} min^{-1}), β is the extent of surface coverage (g mg^{-1}).

2.6.2 Adsorption isotherm models

Langmuir (Eq. 6), Freundlich (Eq. 7), and Temkin (Eq. 8) adsorption isotherm models were used to analyze adsorption equilibria.

$$q_e = (K_l C_e q_m)/(1 + K_l C_e) \quad (6)$$

$$q_e = K_f C_e^{(1/n)} \quad (7)$$

$$q_e = RT/b_T \ln(K_T C_e) \quad (8)$$

Where, qe is the equilibrium adsorbate loaded onto the adsorbent (mg g^{-1}). Ce is heavy metal released (mg L^{-1}) at equilibrium, qm is Langmuir heavy metal adsorption maxima (mg kg^{-1}), Kl is the Langmuir constant (L mg^{-1}) related to metal binding energy, K_f is the Freundlich constant (mg g^{-1}), n is the Freundlich exponent (L kg^{-1}) related to binding energy of metal, R is the universal gas constant (J mol^{-1} K^{-1}), T temperature (Kelvin), A is the equilibrium binding constant (L g^{-1}), b_T is the Temkin constant; B is the (RT/bT); and K_T is the constant related to heat of sorption (J mol^{-1}).

2.6.3 Thermodynamics

Parameters ΔG, ΔH, and ΔS were derived from Van't Hoff equations to interpret spontaneity and heat changes during adsorption.

$$\Delta G = \Delta H - T\Delta S \quad (9)$$

$$\Delta G = -RT \ln K \quad (10)$$

$$\ln K = (\Delta S/R) - (\Delta H/RT) \quad (11)$$

Where, ∆G is change in Gibb's free energy (KJ mol^{-1}); ∆H is change in enthalpy (KJ mol^{-1}); ∆S is change in entropy (J mol^{-1} K^{-1}); T is temperature (K), K is the distribution coefficient of the metal ions between adsorbed phase and the bulk aqueous solution ($K = C_A/C_e$), where $C_A = (C_0 - C_e)$ is the adsorbed quantity of adsorbate (mg L^{-1}) at equilibrium and C_e is the equilibrium concentration (mg L^{-1}) in solution.

OrigingPro9 software® was used to fit experimental data to the non-linear forms of kinetic and isotherm models; Adj. R^2 (Eq. 12) and Chi-square (χ^2) (Eq. 13) were employed to determine the adequacy of these models. All the figures were developed in Microsoft Office Excel 2019.

$$\text{Adj. } R^2 = 1 - [(1 - R^2)(n-1)/(n-1-p)] \quad (12)$$

$$\chi^2 = \sum[(yi - yi')^2/yi'] \quad (13)$$

χ^2 Where, yi is the experimental response for ith observation; yi' is the predicted value of yi; n is the total number of observations and p is the total number of model parameters; reduced χ^2 is the ratio of χ^2 to degrees of freedom.

3. RESULTS AND DISCUSSION

3.1 Characteristics of Ben and Ac-Ben

3.1.1 XRD, SEM-EDX and specific surface area

Bentonite had characteristic XRD peak at 6.9° (2θ) (001 plane), which is corresponding to montmorillonitic structure (Fig. 2). Mild descriptive diffractions were recorded at 20.9° (quartz) and 26.7° (dolomite) due to the presence of clay and non-clay impurities (Sarkar et al. 2021). Disintegration of bentonite structure in acid activated samples resulted in higher alterations in the interval between 5.8° and 21° of 2θ (Krupskaya et al. 2021). Due to thermo-chemical activation of bentonite (Ac-Ben) intensities of the peaks to the raw bentonite (Ben) was dropped (Belhadri et al. 2019). SEM images of Ben showed presence of several flaky, semicircular and circular particles of bentonite particles (Fig. 2). SEM indicated that micro-size particles are made up of individual platelets that aggregate into large-size particles, as demonstrated by high magnification micrograph of the Ac-Ben structure (Fig. 2). These flaky structures could be due to dominance of montmorillonitic minerals in the bentonite. Anna et al. (2014) reported that bentonite powder could contains very high quantity (more than 90%) smectite minerals in its mineralogical composition. Structures of Ac-Ben are irregular in shape and rough enough to favour adsorption (Can et al. 2021). EDX spectrum of Ac-Ben indicates the presence of O, Si, Al, Fe, Cu etc. (Fig. 2). Hebbar et al. (2014) reported that peaks corresponded to Na and Mg of bentonite disappeared due to exchange of Na and Mg with protons. EGME method was used to analyze specific surface area of Ben and Ac-Ben. Ben and Ac-Ben has specific surface area of 91.8 and 153.6 m2 g-1, respectively. It was previously stated that, "EGME has an advantage over gas adsorption method (BET) as it is able to explore the internal surface area of clay minerals (interlayer surfaces), which are relevant under natural environmental conditions but inaccessible under dry situations during the process of gas adsorption" (Heister 2014).

3.1.2 FTIR and point of zero charge (pHPZC)

The FTIR peak (Fig. 3) at 1031 cm^{-1} of raw bentonite was attributed to Si-O stretching vibrations (in-plane) of the tetrahedral sheets, whereas the bands around 533 and 468 cm^{-1} are

attributed to Si-O-Al and Si-O-Si bending vibrations, respectively (Taher et al. 2019). The intensive bands near 913 cm^{-1} assigned to Al-Mg-OH stretching vibration. The raw bentonite spectrum also contains a band at 792 cm^{-1} which indicated the presence of quartz (Thakur et al. 2021). After sulfuric acid activation, the Ac-Ben showed decreasing intensity in the FTIR spectrum that indicates leaching of octahedral cations, such as Al^{3+} and Mg^{2+} from the bentonite structure. The decrease of the content of the octahedral cations is attended with a decrease in OH bending vibrations at 913 cm^{-1} (Ajala et al. 2018). Ac-Ben showed decreasing the intensity of IR spectra throughout the wave number range after Pb(II) and Cd(II) adsorption (Fig. 3). The FTIR result is in clear agreement with the XRD studies which indicate sequential degradation of the bentonite clay sheet upon acid treatment.

The pH_{PZC} of Ben is 7.1 and 7.5 for 0.1 *M* KNO_3 and 0.01 *M* KNO_3, respectively; whereas, pH_{PZC} of Ac-Ben sample was observed at 4.7 and 4.9 for 0.1 *M* and 0.01 *M* KNO_3 solutions, respectively (Fig. 4). If pH < pH_{PZC}, it is assumed that the surface area of the adsorbents is positively charged and while pH > pH_{PZC} the surface area of the adsorbents is negatively charged. For both Ben and Ac-Ben pH > pH_{PZC}, which indicates their surface area are negatively charged, causing deprotonation of the active spots on the adsorbent and binding of Pb(II) and Cd(II) at the given spots in the adsorbent structure (Tang et al. 2019). The thermo-chemical treatment reduced PZC of bentonite (pH_{PZC} 7.3 in Ben to 4.8 in Ac-Ben), which make it favorable to use as adsorbent in wide range of operation for pH than the Ben (Musie and Gonfa 2022).

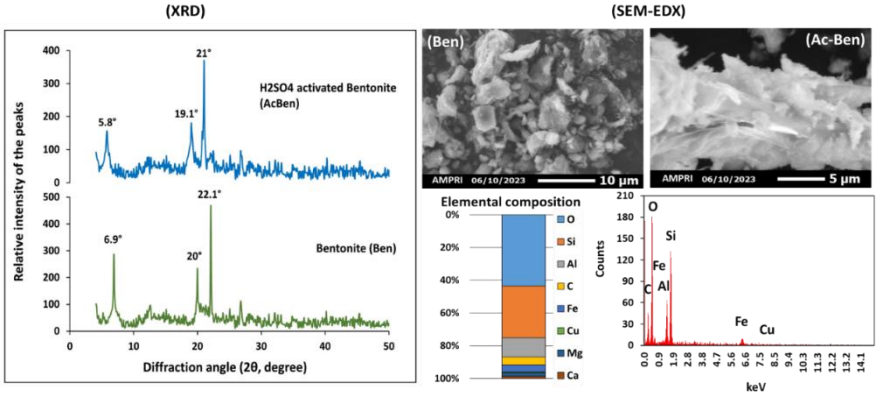

Fig. 2. XRD-patterns and SEM-EDX images of bentonite (Ben) and activated bentonite (Ac-Ben)

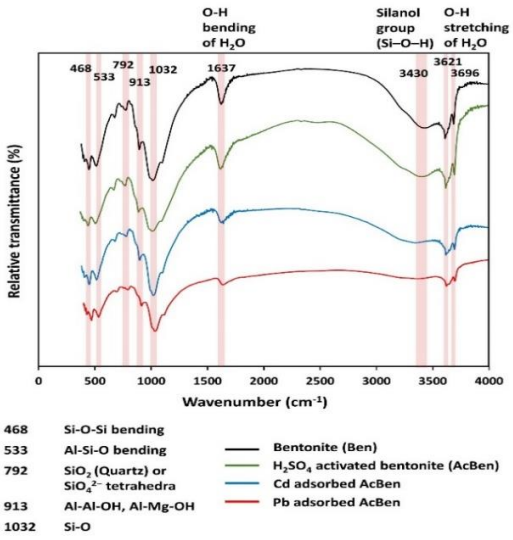

Fig. 3. FTIR spectra of bentonite (Ben), H_2SO_4 activated bentonite (Ac-Ben), Cd(II) adsorbed Ac-Ben, Pb(II) adsorbed Ac-Ben

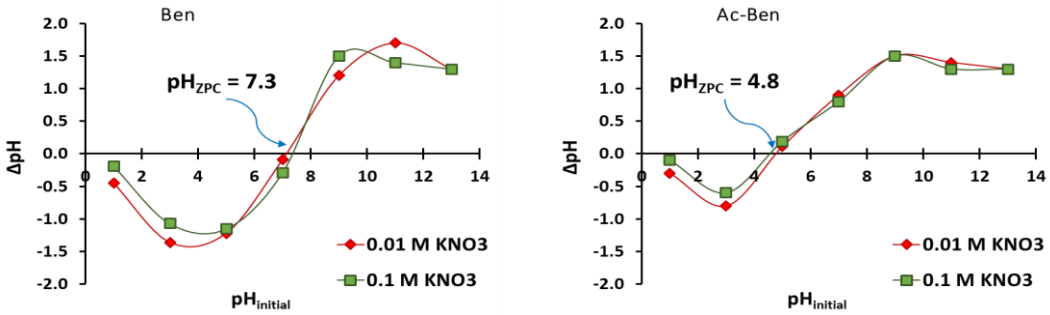

Fig. 4. Point of zero charge (PZC) of Ben and Ac-Ben

3.2 Effects of Different Conditions on Pb (II) and Cd (II) Adsorption

3.2.1 Effects of contact time on Pb (II) and Cd (II) removal

Percent removal of Pb (II) and Cd (II) was attained steady value at 60 min for Ac-Ben; however, removal of Pb (II) and Cd (II) increased with higher shaking time (Fig. 5a). Ac-Ben out performs Ben in terms of time taken to remove both Pb (II) and Cd (II) from the wastewater. Percent removal of Cd (II) increases from 89.4 to 99.6% in Ac-Ben, respectively for 15 to 60 minutes and reaches at its equilibrium. "Abundance of unoccupied binding sites on the external surface of the Ac-Ben are responsible for the rapid adsorption during the initial stage, and subsequently remaining available sites were difficult to be occupied due to repulsive interaction between solute molecules on the solid and bulk phases" (Sarkar et al. 2017). "When saturation was achieved at the external surfaces, then the metal ions would penetrate into the pores of adsorbent and become adsorbed by the particle's internal surfaces" (Siyal et al. 2016).

3.2.2 Effects of adsorbent doses on Pb (II) and Cd (II) removal

The removal efficiency of Pb (II) increased from 69.7 to 87.6% and 85.8 to 98.5% for Ben and Ac-Ben, respectively when the dose is increased from 5 to 30 g L^{-1} (Fig. 5b). Besides, Cd (II) removal efficiency was increased from 76.2 to 89.6% with increasing doses of Ben. "The removal efficiency intensely rises with increasing adsorbent due to the presence of more unoccupied active sites on the surface of Ben and Ac-Ben" (Ali 2018). However, maximum adsorption of Cd (II) (94.8 to 97.9%) ions was observed by Ac-Ben which has no significant changes over its doses. It implies that at low doses, active sites of the adsorbent are adequate to adsorb the entire metal ions present in the solution. Beyond 10 g L-1 of Ac-Ben removal percent of Pb (II) and Cd (II) was correspondingly attained worthy value (>95%). The residual metal ions in bulk remain in equilibrium with the adsorbed metal ions on adsorbent's surface.

3.2.3 Effects of solution pH on Pb (II) and Cd (II) removal

Pb(II) and Cd(II) removal percent increased with the solution pH rise from 3 to 8 (Fig. 5c). The pH of metal ion solution influences both the adsorbent and metal ion by altering the surface and degree of ionization. Beyond pH 4, the removal percent of Cd(II) by Ben was increased continuously to about 88.2% at pH 8. For Ac-Ben Cd(II) and Pb(II) removal percent increased from 91.7 to 99.0% and 88.3 to 97.8% within the pH range from 3 to 8, respectively. At lower pH, the H^+ concentration was higher; and as the solution pH increases, the concentration of H^+ decreases. Thus, "decreasing H^+ competence with Pb(II) and Cd(II) on the adsorbent surface increases adsorption capacity" (Panda et al. 2020). "The adsorbent's surface is saturated with negative charge at high pH values, which promotes the adsorption of positively charged metal ions onto their surface" (Ajala et al. 2018).

3.2.4 Effects of temperature on Pb(II) and Cd(II) removal

Pb(II) and Cd(II) removal percent was decreased with increasing solution temperature from 298 to 318 K (Fig. 5d), which indicates that metal ion adsorption onto adsorbents is physisorption in nature. Ben (91.7% Pb and 91.5% Cd) and Ac-Ben (98.3% Pb and 99.5% Cd) both showed better adsorption percentage for Pb(II) and Cd(II) with decreasing temperature. Weak electrostatic interactions between the metal ions and the adsorbent at elevated temperatures could be the cause of the decrease in adsorption (El Maghrabi et al. 2020). As a result, lowering the temperature is better for non-ionic exchange

adsorption, indicating that the adsorbents removed the heavy metals by undergoing a non-ionic exchange with the heavy metal ions.

3.2.5 Effects of metal ion concentration on Pb(II) and Cd(II) removal

With increasing initial Pb(II) concentration from 5 to 200 mg L^{-1} percent removal was decreased from 69.7 to 59.2% for Ben and from 100 to 63.8% for Ac-Ben (Fig. 6a). Removal percent of Ben and Ac-Ben drops from 72.7% at 1 ppm to about 68.6% at 10 ppm indicated that Cd(II) adsorption decreases on increasing the Cd(II) concentration (Fig. 6b). Therefore, the rate of Cd(II) ions that travels from the bulk solution to the adsorbent particle surface decreases. "Metal ions bind to the adsorbent rapidly at low concentrations through ionic interactions due to the availability of a plenty of adsorption sites" (Nayak et al. 2017; Eleraky et al., 2025). "Adsorption would have theoretically reached to a plateau after all of the binding sites were occupied because of continuous adsorption. Interestingly, there is a consistent drop in the adsorption percentage as the amount of metal ions increases" (Naseem et al. 2019).

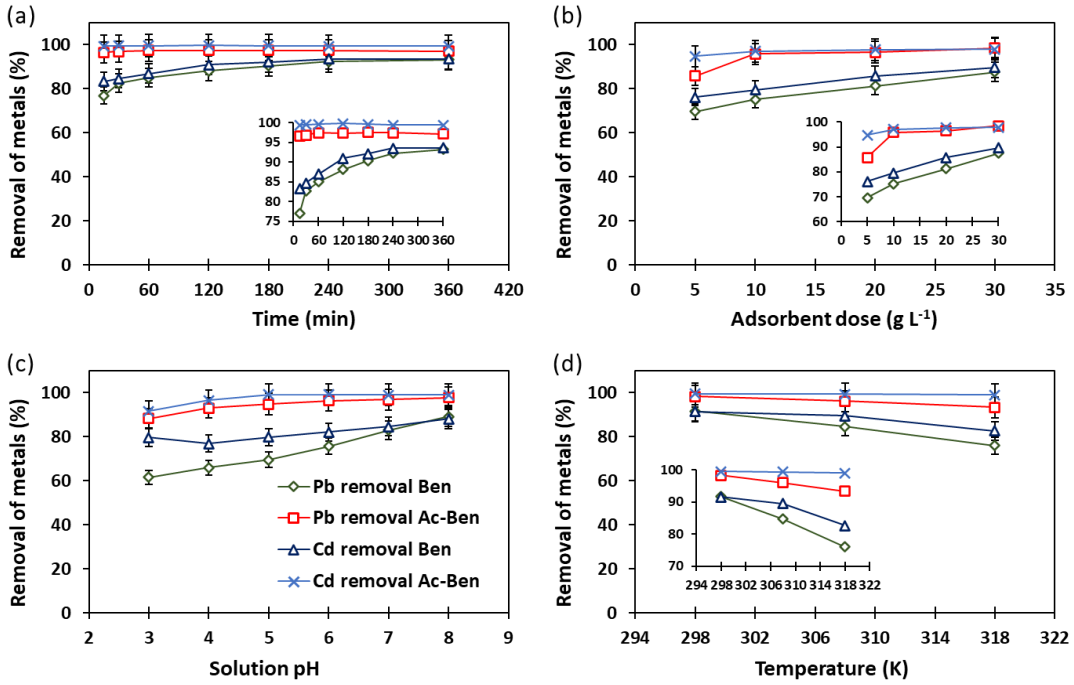

Fig. 5. Effect of contact time (a), adsorbent dose (b), solution pH (c), and temperature (d) on Pb(II) and Cd(II) removal efficiency of Ben and Ac-Ben

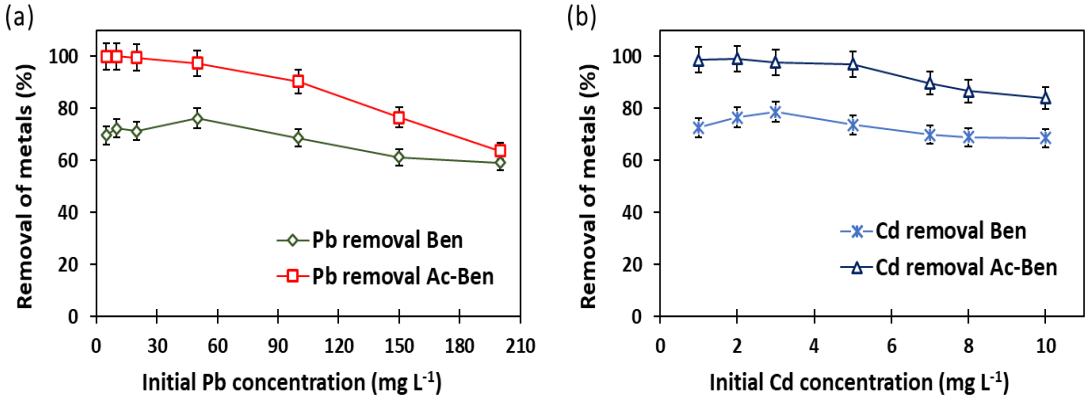

Fig. 6. Effect of initial Pb (a) and Cd (b) ion concentration on Pb(II) and Cd(II) removal efficiency of Ben and Ac-Ben

3.3 Effects on Adsorption Kinetics and Isotherm

"The calculation of adsorption kinetic models (pseudo first-order, pseudo second-order and Elovich kinetic model) is presented in Table 1. Among kinetic models pseudo first-order, pseudo second-order and Elovich kinetic models were well fitted (higher Adj. R^2 and low χ^2 value) to Pb(II) and Cd(II) adsorption on Ben and Ac-Ben. Pseudo first-order kinetic model was best fitted, which indicates predominance of heavy metal physisorption on both Ben and Ac-Ben involving intermolecular van der Waals forces. With increased adsorbate-adsorbent contact time the kinetic trend of Cd(II) and Pb(II) adsorption on Ben and Ac-Ben dropped and reached a plateau. This may be due to proportionally decreased adsorption amount with decreased adsorption capacity of both the adsorbents, which was in agreement with previous reports" (Mukhopadhyay et al. 2019; Sarkar et al. 2022). "The amount of Cd(II) and Pb(II) adsorption increased by prolonging the reaction time. Because electrons are transferred, exchanged, and co-occurring throughout the adsorption process. A number of variables such as the size of the hydrated ions, hydration energy, and the metal ions activity, contributed to the greater amount of Pb(II) adsorption as compared to Cd(II). Additionally, due of Pb(II)'s mobility in the aqueous solution, its activity is also increased" (Das et al. 2021).

Langmuir, Freundlich and Temkin adsorption isotherm were used to find the interaction between the Pb(II), Cd(II) and adsorbent and its degree of adsorption on the adsorbents at constant temperature. "The adsorption of Pb(II) and Cd(II) molecules over the surface of Ben and Ac-Ben having uniform energy sites that are equally available for interaction in the Langmuir model. In the case of Freundlich isotherm, adsorption takes place on a heterogeneous surface in a multilayer" (Manippady et al. 2020). Graphs of metal adsorbed (qt) vs. equilibrium metal conc. The values of qm are calculated from the intercept of the linear plots, which indicates maximum adsorption of the adsorbents. Ben had lower qm values (maximum adsorption capacity) both for Pb(II) and Cd(II) (117 and 92.9 mg g^{-1}, respectively) as compared to the Ac-Ben (127.2 and 132.2 mg g^{-1}, respectively). The adjusted coefficient of determination (Adj. R^2) values of Ben obtained for the Pb(II) and Cd(II) were 0.989 and 0.997, whereas Adj. R^2 values for Ac-Ben for Pb(II) and Cd(II) were 0.996 and 0.999 for Langmuir isotherm (Table 2). When "the concentration of some species in the liquid phase increases, the Freundlich model, which is applicable to heterogeneous surfaces, predicts an increase in the concentration of the ionic species adsorbed on the solid surface" (Araújo et al. 2018). "In Freundlich isotherm model, the values of n are equal or more than 1 indicates favourability of linear adsorption" (Sherugar et al. 2022). The value obtained for Temkin isotherm equilibrium binding constant (A, L g^{-1}) 0.123 (Pb on Ben), 0.139 (Pb on Ac-Ben), 0.885 (Cd on Ben) and 0.961 (Cd on Ac-Ben). Since the bonding energy value was less than 8 kJ mol^{-1}, physical adsorption is the mechanism at play. Because "the adsorbate in the physisorption process adhere to the adsorbent via weak van der Waals interactions, this process is linked to comparatively low adsorption energies" (Araújo et al. 2018; Baari et al., 2025). Table 3 lists previous studies conducted by different researchers on the removal of Pb(II) and Cd(II) using alternative affordable adsorbents.

3.4 Effects on Thermodynamics of Pb(II) and Cd(II) Adsorption

The nature and dimensions of thermodynamic parameters show a mechanism pertaining to the creation of an adsorbed layer and demonstrate the viability of the adsorption process. The results for the thermodynamic parameters obtained for Ben and Ac-Ben are reported in Table 4. Both of the adsorbents presented negative values for ΔG, endorsing that the Pb(II) and Cd(II) adsorption process is spontaneous and thermodynamically favorable. The ΔG value increased with an increase in temperature from 298 K to 318 K that indicated that the adsorption is more favorable at lower temperatures. The degree of spontaneity decreases with the increased temperature which may resulted due to physisorption rather than chemisorption. This result is aligned with findings of Taha et al. (2016) who tested adsorption of Pb(II), Cd(II), and Ni(II) onto Egyptian Na-activated bentonite. Moreover, adsorbate may desorb from the adsorbent's surface at higher temperatures due to the kinetic energy of the adsorbate suppressed the forces of adsorption. In other way, a higher driving force for adsorption is indicated by a more negative ΔG values, which leads to an increased adsorption capacity. Cd(II) adsorption on Ac-Ben is comparatively more favourable than the Pb(II). The ΔS values were 0.155 and 0.101 KJ mol^{-1} K^{-1} for adsorption of Pb(II) and Cd(II) on Ben; whereas, ΔS values

Table 1. Estimated kinetic model parameters for Pb(II) and Cd(II) adsorption onto the bentonite (Ben) and activated bentonite (Ac-Ben) Model Parameters

Model	Parameters		Metals			
			Pb(II)		Cd(II)	
			Ben	Ac-Ben	Ben	Ac-Ben
Pseudo first order	Output	q_e (mg g^{-1})	3.833	4.859	0.236	0.297
		k_1 (min^{-1})	0.144	0.099	0.257	0.151
	Statistics	Reduced χ^2	2.67E-03	1.99E-03	2.85E-05	1.80E-05
		Adj. R^2	0.999	0.999	0.996	0.998
Pseudo second order	Output	q_e (mg g^{-1})	4.983	5.018	0.251	0.333
		k_2 (g mg^{-1} min^{-1})	0.051	0.047	0.382	0.192
	Statistics	Reduced χ^2	1.40E-02	1.27E-02	1.84E-04	7.18E-06
		Adj. R^2	0.995	0.996	0.974	0.999
Elovich kinetic model	Output	α (mg g^{-1} min^{-1})	1.166	3.275	0.802	2.533
		β (g mg^{-1})	3.697	1.463	5.415	2.076
	Statistics	Reduced χ^2	5.26E-02	5.33E-02	4.95E-04	3.99E-05
		Adj. R^2	0.982	0.981	0.930	0.996

Ben: Bentonite; Ac-Ben: Activated bentonite; q_t and q_e are the amount of metal adsorbed (mg g^{-1}) at time t and at equilibrium, k_1 is the rate constant of the pseudo-first order (min^{-1}), t is the time (min), k_2 is the rate constant of the pseudo-second order (g mg^{-1} min^{-1}), α is the initial rate of adsorption (mg g^{-1} min^{-1}), β is the extent of surface coverage (g mg^{-1})

Table 2. Estimated adsorption isotherm model parameters for Pb(II) and Cd(II) adsorption onto the bentonite (Ben) and activated bentonite (Ac-Ben)

Model		Parameter	Metals			
			Pb(II)		Cd(II)	
			Ben	Ac-Ben	Ben	Ac-Ben
Langmuir isotherm	Output	q_m (mg g^{-1})	117.0	127.2	92.9	132.2
		K_l (L mg^{-1})	7.76E-05	0.005	1.60E-03	1.58E-04
	Statistics	Reduced χ^2	0.453	0.101	2.41E-04	3.89E-06
		Adj. R^2	0.989	0.996	0.997	0.999
Freundlich isotherm	Output	K_f (mg g^{-1}) (mg^{-1})$^{1/n}$	0.094	0.278	0.067	0.099
		n	1.019	1.363	1.032	1.409
	Statistics	Reduced χ^2	0.539	0.471	1.83E-04	4.57E-06
		Adj. R^2	0.987	0.982	0.997	0.999
Temkin isotherm	Output	A (L g^{-1})	0.123	0.139	0.885	0.961
		b_T (KJ mol^{-1})	0.613	0.733	4.507	6.902
	Statistics	Reduced χ^2	6.826	1.891	5.43E-03	8.62E-03
		Adj. R^2	0.834	0.930	0.929	0.928

Ben: Bentonite; Ac-Ben: Activated bentonite; qe is the equilibrium adsorbate loaded onto the adsorbent (mg g^{-1}). Ce is heavy metal released (mg L^{-1}) at equilibrium, q_m is Langmuir heavy metal adsorption maxima (mg kg^{-1}), K_l is the Langmuir constant (L mg^{-1}) related to metal binding energy, K_f is the Freundlich constant (mg g^{-1}), n is the Freundlich exponent (L kg^{-1}) related to binding energy of metal, R is the universal gas constant (J mol^{-1} K^{-1}), T temperature (Kelvin), A is the equilibrium binding constant (L g^{-1}), b_T is the Temkin constant; B is the (RT/b_T); and K_T is the constant related to heat of sorption (J mol^{-1}).

Table 3. Comparing maximum adsorption capacity (qmax) of adsorbents of present work with other literatures for Pb(II) and Cd(II) removal

Adsorbents	q_{max} (mg g^{-1})		References
	Pb(II)	Cd(II)	
Metakaolin based Geopolymer	-	70.3	Lan et al. (2019)
Polyethylene glycol bentonite	22.0	18.0	Seilkhanova et al. (2019)
Carboxymethyl β-cyclodextrin bonded Fe_3O_4@SiO_2–NH_2 core-shell magnetic nanocomposite	170.0	-	Jahanbakhsh et al. (2021)
Calcium calcined bentonite clay	32.2	20.3	Meneguin et al. (2017)
$NHCH_3$ treated bentonite	52.1	26.1	Kostenko et al. (2019)
Bentonite-Fe_3O_4-MnO_2	-	33.4	Jiang et al. (2018)
Modified clay composite	172.4	9.15	Teğin et al. (2023)
Humic acid-iron-columnar bentonite (HA-Fe-PILC)	95.3	31.4	Xu et al. (2021)
Bentonite (Ben)	117.0	92.9	Present study
Thermo-chemical activated bentonite (Ac-Ben)	127.2	132.2	Present study

Table 4. Estimated thermodynamic parameters for Pb(II) and Cd(II) adsorption onto the bentonite (Ben) and activated bentonite (Ac-Ben)

Adsorbents	Thermodynamic parameters	Metals					
		Pb(II)			Cd(II)		
	Temperature (K)	298	308	318	298	308	318
Bentonite (Ben)	ΔG (KJ mol^{-1})	-5.960	-4.238	-2.855	-5.877	-5.315	-3.859
	ΔH (KJ mol^{-1})	-52.18			-36.09		
	ΔS (KJ mol^{-1} K^{-1})	0.155			0.101		
	R^2	0.996			0.939		
Activated bentonite (Ac-Ben)	ΔG (KJ mol^{-1})	-10.110	-8.037	-6.576	-13.346	-12.707	-11.618
	ΔH (KJ mol^{-1})	-62.67			-39.18		
	ΔS (KJ mol^{-1} K^{-1})	0.098			0.086		
	R^2	0.990			0.978		

were 0.098 and 0.086 KJ mol^{-1} K^{-1} for adsorption of Pb(II) and Cd(II) on Ac-Ben. "This indicates increased randomness of ions with raised temperature and resulted decreased adsorption of ions. The solid-liquid interface exhibits structural alterations, as suggested by the positive ΔS values found for both the materials" (Panda et al. 2020). "The negative values of ΔH illustrates exothermic adsorption of Cd(II) and Pb(II) ions on SABC and Ac-Ben (Table 4). An exothermic reaction occurs during adsorption with non-ionic exchange. The adsorption is preferred at lower temperature through the physisorption method" (Tran et al. 2016). When the change in ΔH is less than 21 KJ mol^{-1}, it means that during the adsorption process, physical adsorption is resilient than chemisorption. The phenomena involved in these processes are still not completely assumed. The literature states that metallic ions reach the adsorbent's surface through exothermic processes in order to adsorb ions in the aqueous phase.

3.5 Desorption and Reusability Performances

The reusability results (Fig. 7) showed that after three adsorption-desorption cycles the adsorption efficiency of both Ben and Ac-Ben were reduced as compared to their original maximum adsorption efficiency. This can be attributed to lower recovery of bounded metal ions during desorption process, which reduces the number of active adsorption sites available on the adsorbent's surface. In the first cycle, the removal efficiency by Ben was 68.2% for Pb(II) and 76.7% for Cd(II). After three subsequent adsorption-desorption cycles, Ben retained adsorption efficiency up to 47.3 and 52.1% for Pb(II) and Cd(II), respectively. However, a trifling change (98.4% to 69.9% for Pb and 97.9% to 84.3% for Cd) in the adsorption ability of Ac-Ben was observed after three successive adsorption-desorption cycles, which confirms that the AC-Ben have great potential for renewal and subsequent reuse as adsorbent materials as compared the Ben. Further, adsorption-desorption studies led with higher concentration of desorbing agents may results more efficient recovery of metals and successful adsorbents renewal.

3.6 Mechanism of Pb(II) and Cd(II) Adsorption for Ac-Ben

Fig. 8 depicts a schematic representation of the proposed adsorption mechanisms between Pb(II), Cd(II), and Ac-Ben. The breakdown of the smectite structure and the significant substitution of H^+ for cations increase the surface area of bentonite during the thermo-chemical activation process (Guan et al. 2022). FTIR, XRD, SEM, and EDX analyses have demonstrated that these transformations in the montmorillonite and illitic layers result in notable changes in the cation exchange capacity, chemical, and mineralogical properties of bentonite. The removal mechanism of Ac-Ben is significant because it may be related to its higher electronegativity and its structural composition, which consists of two silica tetrahedral and one alumina octahedral sheets (Dhar et al. 2023). This composition holds a net negative charge, which indicates broken bonds at the edges of the aluminum-silica units, which ultimately result in unsatisfied charges that can be balanced by the cation exchange.

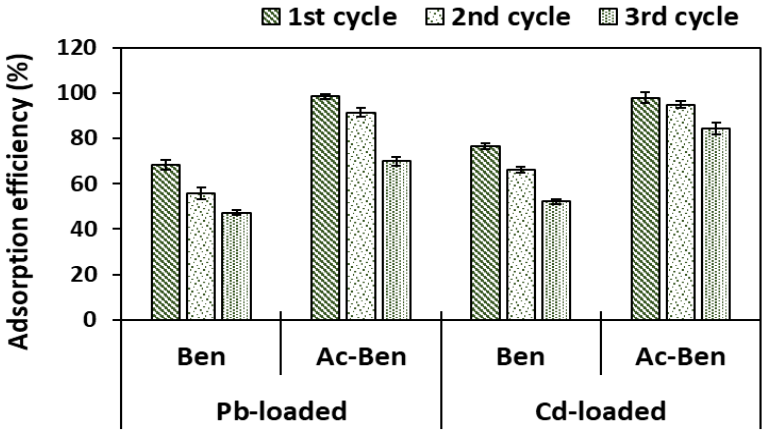

Fig. 7. Pb(II) and Cd(II) adsorption capacities and reusabilities of Ben and Ac-Ben after three consecutive adsorption-desorption cycles

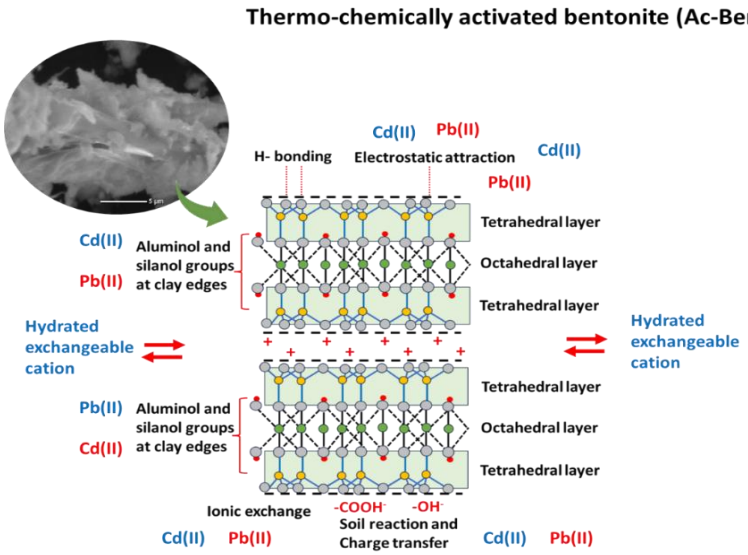

Fig. 8. Proposed mechanisms of Pb(II) and Cd(II) adsorption on Ac-Ben

4. CONCLUSION

This study demonstrates that thermo-chemically activated bentonite (Ac-Ben) is a highly effective adsorbent for the removal of Pb(II) and Cd(II) from aqueous solutions. Compared to raw bentonite, Ac-Ben exhibited improved physicochemical properties, higher adsorption capacity, and better reusability. The adsorption process followed pseudo-first-order kinetics and Langmuir isotherm, suggesting monolayer physical adsorption. Thermodynamic analysis confirmed spontaneity and exothermic nature. Ac-Ben retained high efficiency over multiple cycles, highlighting its potential for sustainable wastewater treatment. Its low cost, simplicity of preparation, and high performance make Ac-Ben a promising solution for heavy metal remediation in alignment with sustainable development goals.

The adoption of the natural waste materials viz. bentonite represents a sustainable, inclusive, and economically viable approach to wastewater treatment, particularly for heavy metal removal by minimizing reliance on synthetic materials and reducing waste. Continued research can enhance their efficiency, scalability, and societal impact, contributing to global efforts in environmental conservation and water security.

CONSENT

This is an original article and all the data presented are primary data generated by the authors. Due citation of previous article is provided within the manuscript.

DISCLAIMER (ARTIFICIAL INTELLIGENCE)

Author(s) hereby declare that generative AI technologies such as Large Language Models ChatGPT version 3.5 has been used during writing or editing of this manuscript.

ACKNOWLEDGEMENT

The authors would like to acknowledge technical and management support from ICAR-Indian Institute of Soil Science, Bhopal for providing internal facilities for this research work. The authors would also sincerely acknowledge CSIR-Advanced Materials and Process Research Institute (AMPRI), Bhopal, India for providing instrument facilities.

COMPETING INTERESTS

Authors have declared that no competing interests exist.

REFERENCES

Ajala, O.J., Nwosu, F.O., & Ahmed, R.K. (2018). Adsorption of atrazine from aqueous solution using unmodified and modified bentonite clays. Applied Water Science, 8, 1–11. https://doi.org/10.1007/s13201-018-0855-y

Ali, M.E. (2018). Synthesis and adsorption properties of chitosan-CDTA-GO nanocomposite for removal of hexavalent chromium from aqueous solutions. Arabian

Journal of Chemistry, 11, 1107e1116. https://doi.org/10.1016/j.arabjc.2016.09.010

Anna, B., Kleopas, M., Constantine, S., Anestis, F., & Maria, B. (2014). Adsorption of Cd(II), Cu(II), Ni(II) and Pb(II) onto natural bentonite: study in mono- and multi-metal systems. Environmental Earth Sciences, 73, 5435-5444. https://doi:10.1007/s12665-014-3798-0

Araújo, C.S.T., Almeida, I.L.S., Rezende, H.C., Marcionilio, S.M.L.O., Léon, J.J.L., & de Matos, T.N. (2018). Elucidation of mechanism involved in adsorption of Pb(II) onto lobeira fruit (Solanum lycocarpum) using Langmuir, Freundlich and Temkin isotherms. Microchemical Journal, 137, 348-354. https://doi:10.1016/j.microc.2017.11.009

Baari, M. J., Rudi, L., & Harimu, L. (2025). Adsorption isotherms, thermodynamics, and kinetics of activated carbon as adsorbent to water pollutants: a review. Chimica Techno Acta, 12(2), 12214. https://doi.org/10.15826/chimtech.2025.12.2.14

Babaki, H., Salem, A., & Jafarizad, A. (2008). Kinetic model for the isothermal activation of bentonite by sulfuric acid. Materials Chemistry and Physics, 108, 263-268. https://doi.org/10.1016/j.matchemphys.2007.09.034

Belhadri, M., Mokhtar, A., Meziani, S., Sassi, M., & Bengueddach, A. (2019). Novel low-cost adsorbent based on economically modified bentonite for lead(II) removal from aqueous solutions. Arabian Journal of Geosciences, 12, 88. https://doi.org/10.1007/s12517-019-4232-4

Can, H.K., Sevim, H., Şahin, Ö., & Gürpınar, Ö.A. (2021). Experimental routes of cytotoxicity studies of nanocomposites based on the organo-bentonite clay and anhydride containing co-and terpolymers. Polymer Bulletin, 79, 5549-5567. https://doi.org/10.1007/s00289-021-03776-w

Carter, D.L., Mortland, M.M., & Kemper, W.D. (1986). Specific Surface. In: Klute A (ed) Methods of Soil Analysis: Part 1 Physical and Mineralogical Methods (2nd ed.). American Society of Agronomy, Wiley, New York, pp 413-423. https://doi.org/10.2136/sssabookser5.1.2ed.c16

Das, L., Saha, N., Ganguli, A., Das, P., Bhowal, A., & Bhattacharjee, C. (2021). Calcium alginate-bentonite/activated biochar composite beads for removal of dye and Biodegradation of dye-loaded composite after use: Synthesis, removal, mathematical modeling and biodegradation kinetics. Environmental Technology & Innovation, 24, 101955. https://doi.org/10.1016/j.eti.2021.101955

Dhar, A.K., Himu, H.A., Bhattacharjee, M., Mostufa, M.G., & Parvin, F. (2023). Insights on applications of bentonite clays for the removal of dyes and heavy metals from wastewater: a review. Environmental Science and Pollution Research, 30, 5440-5474. https://doi.org/10.1007/s11356-022-24277-x

El Maghrabi, A.H., Marzouk, M.A., Elbably, M.A., & Hassouna, M.E.M. (2020). Biosorption of manganese by amended Aspergillus versicolor from polluted water sources. Nature Environment and Pollution Technology, 9, 1645-1656. https://doi.org/10.46488/NEPT.2020.v19i04.000

Eleraky, M. I., Razek, T. M., Hasani, I. W., & Fahim, Y. A. (2025). Adsorptive removal of lead, copper, and nickel using natural and activated Egyptian calcium bentonite clay. Scientific Reports, 15(1), 13050. https://doi.org/10.1038/s41598-025-95184-7

Gorgievski, M., Božić, D., Stanković, V., Štrbac, N., & Šerbula, S. (2013). Kinetics equilibrium and mechanism of Cu2+, Ni2+ and Zn2+ ions biosorption using wheat straw. Ecological Engineering, 58, 113-121. https://doi.org/10.1016/j.ecoleng.2013.06.025

Guan, X., Yuan, X., Zhao, Y., Bai, J., Li, Y., Cao, Y., Chen, Y., & Xiong, T. (2022). Adsorption behaviors and mechanisms of Fe/Mg layered double hydroxide loaded on bentonite on Cd (II) and Pb (II) removal. Journal of Colloid and Interface Science, 612, 572-583. https://doi.org/10.1016/j.jcis.2021.12.151

Hebbar, R.S., Isloor, A.M., Ismail, & A.F. (2014). Preparation and evaluation of heavy metal rejection properties of polyetherimide/porous activated bentonite clay nanocomposite membrane. RSC Advances, 4(88), 47240-47248. https://doi.org/10.1039/C4RA09018G

Heister, K. (2014). The measurement of the specific surface area of soils by gas and polar liquid adsorption methods-Limitations

and potentials. Geoderma, 216, 75-87. https://doi.org/10.1016/j.geoderma.2013.10.015

Hussain, M.I., Muscolo, A., Farooq, M., & Ahmad, W. (2019). Sustainable use and management of non-conventional water resources for rehabilitation of marginal lands in arid and semiarid environments. Agricultural Water Management, 221, 462–476. https://doi.org/10.1016/j.agwat.2019.04.014

Jahanbakhsh, Z., Hosseinzadeh, H., & Masoumi, B. (2021). Synthesis of carboxymethyl β-cyclodextrin bonded Fe3O4@ SiO2–NH2 core-shell magnetic nanocomposite adsorbent for effective removal of Pb (II) from wastewater. Journal of Sol-Gel Science and Technology, 99, 230-242. https://doi.org/10.1007/s10971-021-05569-z

Jiang, L., Ye, Q., Chen, J., Chen, Z., & Gu, Y. (2018). Preparation of magnetically recoverable bentonite–Fe3O4–MnO2 composite particles for Cd(II) removal from aqueous solutions. Journal of Colloid and Interface Science 513, 748-759. https://doi:10.1016/j.jcis.2017.11.063

Khanam, R., Kumar, A., Nayak, A.K., Shahid, M., Tripathi, R., Vijayakumar, S., & Chatterjee, D. (2020). Metal (loid) (As, Hg, Se, Pb and Cd) in paddy soil: bioavailability and potential risk to human health. Science of the Total Environment, 699, 134330. https://doi.org/10.1016/j.scitotenv.2019.134330

Kostenko, L.S., Tomashchuk, I.I., Kovalchuk, T.V., & Zaporozhets, O.A. (2019). Bentonites with grafted aminogroups: Synthesis, protolytic properties and assessing Cu(II), Cd(II) and Pb(II) adsorption capacity. Applied Clay Science, 172, 49-56. https://doi:10.1016/j.clay.2019.02.009

Krupskaya, V., Novikova, L., Tyupina, E., Belousov, P., Dorzhieva, O., Zakusin, S., Kim, K., Roessner, F., Badetti, E., & Brunelli, A. (2019). The influence of acid modification on the structure of montmorillonites and surface properties of bentonites. Applied Clay Science, 172, 1-10. https://doi.org/10.1016/j.clay.2019.02.001

Lan, T., Li, P., Rehman, F.U., Li, X., Yang, W., & Guo, S, (2019). Efficient adsorption of Cd2+ from aqueous solution using metakaolin geopolymers. Environmental Science and Pollution Research, 26, 33555-33567. https://doi.org/10.1007/s11356-019-06362-w

Manippady, S.R., Singh, A., Basavaraja, B.M., Samal, A.K., Srivastava, S., & Saxena, M. (2020). Iron–carbon hybrid magnetic nanosheets for adsorption-removal of organic dyes and 4-nitrophenol from aqueous solution. ACS Applied Nano Materials, 3, 1571-1582. https://doi.org/10.1021/acsanm.9b02348

Meneguin, J.G., Moisés, M.P., Karchiyappan, T., Faria, S.H.B., Gimenes, M.L., de Barros, M.A.S.D., & Venkatachalam, S. (2017). Preparation and characterization of calcium treated bentonite clay and its application for the removal of lead and cadmium ions: Adsorption and thermodynamic modeling. Process Safety and Environmental Protection, 111, 244.252. https://doi:10.1016/j.psep.2017.07.005

Minhas, P.S., Saha, J.K., Dotaniya, M.L., Sarkar, A., & Saha, M. (2022). Wastewater irrigation in India: Current status, impacts and response options. Science of the Total Environment, 808, 152001. https://doi.org/10.1016/j.scitotenv.2021.152001

Mukhopadhyay, R., Adhikari, T., Sarkar, B., Barman, A., Paul, R., Patra, A.K., Sharma, P.C., & Kumar, P. (2019). Fe-exchanged nano-bentonite outperforms Fe3O4 nanoparticles in removing nitrate and bicarbonate from wastewater. Journal of Hazardous Materials, 376, 141-152. https://doi.org/10.1016/j.jhazmat.2019.05.025

Naeem, M.A., Imran, M., Amjad, M., Abbas, G., Tahir, M., Murtaza, B., Zakir, A., Shahid, M., Bulgariu, L., & Ahmad, I. (2019). Batch and column scale removal of cadmium from water using raw and acid activated wheat straw biochar. Water, 11, 1438. https://doi.org/10.3390/w11071438

Nag, R., & Cummins, E. (2022). Human health risk assessment of lead (Pb) through the environmental-food pathway. Sci Tot Environ 810, 151168. https://doi.org/10.1016/j.scitotenv.2021.151168

Naseem, K., Begum, R., Wu, W., Usman, M., & Farooqi, J.H. (2019). Adsorptive removal of heavy metal ions using polystyrene-poly (N-isopropylmethacrylamide-acrylic acid) core/shell gel particles: adsorption

isotherms and kinetic study. Journal of Molecular Liquids, 277, 522-531. https://doi.org/10.1016/j.molliq.2018.12.054

Nayak, B., Samant, A., Patel, R.K., & Misra, P.K. (2017). Comprehensive understanding of the kinetics and mechanism of fluoride removal over a potent nano crystalline hydroxyapatite surface. ACS Omega, 2, 8118-8128. https://doi.org/10.1021/acsomega.7b00370

Nwosu, F.O., Ajala, O.J., Okeola, F.O., Adebayo, S.A., Olanlokun, O.K., Eletta, & O.A.A. (2019). Adsorption of chlorotriazine herbicide onto unmodified and modified kaolinite: equilibrium, kinetic and thermodynamic studies. Egyptian Journal of Aquatic Research, 45, 99-107. https://doi.org/10.1016/j.ejar.2019.05.005

Panda, L., Jena, S.K., Rath, S.S., & Misra, P.K. (2020). Heavy metal removal from water by adsorption using a low-cost geopolymer. Environmental Science and Pollution Research, 27, 24284-24298. https://doi.org/10.1007/s11356-020-08482-0

Sarkar, A., Biswas, D.R., Datta, S.C., Dwivedi, B.S., Bhattacharyya, R., Kumar, R., Bandyopadhyay, K.K., Saha, M., Chawla, G., Saha, J.K., & Patra, A.K. (2021). Preparation of novel biodegradable starch/poly(vinyl alcohol)/bentonite grafted polymeric films for fertilizer encapsulation. Carbohydrate Polymers, 259, 117679. https://doi.org/10.1016/j.carbpol.2021.117679

Sarkar, A., Saha, M., Saha, J.K., Coumar, M.V. Mandal, A., & Patra, A.K. (2022). Comparative assessment of P adsorption, release kinetics, enzymatic activities of weathered fly ash amended texturally different soils. International Journal of Environmental Science and Technology, 19, 2089-2106. https://doi.org/10.1007/s13762-021-03196-3

Sarkar, C., Basu, J.K., & Samanta, A. (2017). Removal of Ni2+ ion from waste water by geopolymeric adsorbent derived from LD slag. Journal of Water Process Engineering, 17, 237-244. https://doi.org/10.1016/j.jwpe.2017.04.012

Shahrokhi-Shahraki, R., Benally, C., El-Din, M.G., & Park, J. (2020). High-efficiency removal of heavy metals using tire-derived activated carbon vs commercial activated carbon: insights into the adsorption mechanisms. Chemosphere, 264, 128455. https://doi.org/10.1016/j.chemosphere.2020.128455

Sherugar, P., Padaki, M., Naik, N.S., George, S.D., & Murthy, D.H.K. (2022). Biomass-derived versatile activated carbon removes both heavy metals and dye molecules from wastewater with near-unity efficiency: mechanism and kinetics. Chemosphere, 287, 132085. https://doi.org/10.1016/j.chemosphere.2021.132085

Siyal, A., Azizli, K.A., Ismail, L., Man, Z., & Khan, M.I. (2016). Suitability of Malaysian fly ash for geopolymer synthesis. Advanced Materials Research, 1133, 201-205. https://doi.org/10.4028/www.scientific.net/AMR.1133.201

Sriram, G., Bhat, M.P., Kigga, M., Uthappa, U.T., Jung, H.Y., Kumeria, T., & Kurkuri, M.D. (2019). Amine activated diatom xerogel hybrid material for efficient removal of hazardous dye. Materials Chemistry and Physics, 235, 121738. https://doi.org/10.1016/j.matchemphys.2019.121738

Taha, A.A., Shreadah, M.A., Ahmed, A.M., & Heiba, H.F. (2016). Multi-component adsorption of Pb(II), Cd(II), and Ni(II) onto Egyptian Na-activated bentonite; equilibrium, kinetics, thermodynamics, and application for seawater desalination. Journal of Environmental Chemical Engineering, 4, 1166-1180. https://doi:10.1016/j.jece.2016.01.025

Taher, T., Rohendi, D., Mohadi, R., & Lesbani, A. (2019). Congo red dye removal from aqueous solution by acid-activated bentonite from sarolangun: kinetic, equilibrium, and thermodynamic studies. Arab Journal of Basic and Applied Sciences, 26, 125-136. https://doi.org/10.1080/25765299.2019.1576274

Tang, Q., Shi, C., Shi, W., Huang, X., Ye, Y., Jiang, W., Kang, J., Liu, D., Ren, Y., & Li, D. (2019). Preferable phosphate removal by nano-La (III) hydroxides modified mesoporous rice husk biochars: Role of the host pore structure and point of zero charge. Science of the Total Environment, 662, 511-520. https://doi.org/10.1016/j.scitotenv.2019.01.159

Teğin, I., Batur, M.Ş., Yavuz, Ö., & Saka, C. (2023). Removal of Cu (II), Pb (II) and Cd (II) metal ions with modified clay

composite: kinetics, isotherms and thermodynamics studies. International Journal of Environmental Science and Technology, 20, 1341-1356. https://doi.org/10.1007/s13762-022-04028-8

Thakur, A.K., Kumar, R., Chaudhari, P., & Shankar, R. (2021). Removal of heavy metals using bentonite clay and inorganic coagulants. In: Shah MP (ed) Removal of Emerging Contaminants Through Microbial Processes. Springer, Singapore. https://doi.org/10.1007/978-981-15-5901-3_3

Tran, H.N., You, S., & Chao, H. (2016). Thermodynamic parameters of cadmium adsorption onto orange peel calculated from various methods: a comparison study. Journal of Environmental Chemical Engineering, 4, 2671-2682. https://doi.org/10.1016/j.jece.2016.05.009

Ungureanu, N., Vladut, V., & Voicu, G. (2020). Water scarcity and wastewater reuse in crop irrigation. Sustainability, 12, 9055. https://doi.org/10.3390/su12219055

Xu, H., Hu, X., Chen, Y., Li, Y., Zhang, R., Tang, C., & Hu, X. (2021). Cd(II) and Pb(II) absorbed on humic acid-iron-pillared bentonite: Kinetics, thermodynamics and mechanism of adsorption. Colloids and Surfaces A: Physicochemical and Engineering Aspects, 612, 126005. https://doi:10.1016/j.colsurfa.2020.12600

Peer-review history:
The peer review history for this paper can be accessed here:
https://pr.sdiarticle5.com/review-history/135820